Atomic Scale Observations of Metal-Induced Gap States at {222} MgO/Cu Interfaces

D. A. Muller,[1,2] D. A. Shashkov,[3] R. Benedek,[3] L. H. Yang,[4] J. Silcox,[1] and D. N. Seidman[3]
[1]*School of Applied and Engineering Physics, Cornell University, Ithaca, New York 14853*
[2]*Bell Laboratories, Lucent Technologies, Murray Hill, New Jersey 07974*
[3]*Department of Materials Science and Engineering, Northwestern University, Evanston, Illinois 60208*
[4]*Condensed Matter Physics Division, Lawrence Livermore National Laboratory, Livermore, California 94551*
(Received 9 October 1997)

{222} MgO/Cu interfaces produced by internal oxidation are studied by electron energy loss spectroscopy (EELS) using an atomic sized electron beam. We determine interfacial chemistry of this interface with subnanometer spatial resolution and use EELS to measure directly the electronic states pertaining to the buried interface. O, K, and Cu $L_{2,3}$ edges show the formation of metal-induced states within the band gap of MgO, at the interface (which we find to be O terminated). Both experiment and *ab initio* calculations find the metal-induced gap states to be strongly localized at the interface, resulting in a very small interface core-level shift. [S0031-9007(98)06197-3]

PACS numbers: 73.20.–r, 61.16.Bg, 68.35.Dv, 82.65.Dp

A ceramic/metal interface is the extreme example of a boundary between dissimilar materials [1]. Simple models of metals and wide-band gap insulators often emphasize very different physics (delocalized electron bands vs point ions), making it very difficult to capture the microscopic details of the interfaces. In this Letter, we examine the composition and electronic structure of {222} MgO/Cu internal interfaces using electron energy loss spectroscopy (EELS) with a finely focused probe (0.2–0.5 nm). We report observations of metal-induced gap states (MIGS) concentrated at the interface that greatly reduce the charge redistribution and band bending relative to a typical semiconductor/metal interface. This contrasts with the conclusions drawn if only electronegativity arguments are considered. The effect can be very important for transport properties across gate oxides in transistors and for the mechanical behavior of composite materials: adhesion at ceramic/metal interfaces often controls the mechanical properties. Finally, we note that this is an example in which the electronic structure and screening of a bulk interface is very different from the free surface or a monolayer of metal on the oxide [2,3], even when the local atomic arrangements are very similar.

That the internal and free surfaces are different is not unexpected: at a free surface, the neutral (001) MgO surface is the most stable, resulting in a cubic equilibrium crystal shape. However MgO precipitates formed in Cu are octahedral and have {222} facets [4], which are polar, and not stable as free surfaces. There are two possible terminations for the {222} MgO/Cu interface, Mg-Cu or O-Cu. Cu-O termination has been indirectly inferred from matching simulations to high-resolution transmission electron microscopy (HRTEM) [5] and directly from atom-probe field-ion microscopy [6]. Density functional calculations [7] find that Cu-O terminations are energetically favored over Cu-Mg terminations.

Atomically clean {222} MgO/Cu interfaces for this study were produced by internally oxidizing a Cu 2.5 at. % Mg alloy for 2 h at 1223 K in a Rhines pack [8] which yields precipitates, 10 to 30 nm in diameter. Advantages of this approach are (i) clean interfaces with negligible impurity segregation because of the large total interface area to volume ratio [6], (ii) common low-index directions between MgO and Cu, with interplanar spacings suitable for HRTEM, and (iii) a large number of interfaces suitable for electron microscopy are present—we examined 50 interfaces from 16 grains. Specimens were electropolished to produce electron-transparent thin areas and then ion milled for 10 min to reduce surface contamination levels. For the EELS studies, a VG-HB501 100 kV scanning transmission electron microscope (STEM) equipped with a cold-field-emission gun and a McMullan-style parallel EELS spectrometer [9] was used. The spectrometer resolution was set at 1 eV to increase the signal/background ratio. The microscope has been modified to achieve high energy-drift stability (<0.2 eV min^{-1}) and spatial-drift stability (<0.05 nm min^{-1}) [10]. The minimum attainable probe size of this instrument is ≈ 0.22 nm. The EELS spectra were recorded simultaneously with the annular dark field (ADF) signal, under conditions optimized for atomic resolution imaging [11–14]: the objective and collector apertures are 10 and 16 mrad, respectively.

The O-K, Mg-K, and Cu $L_{2,3}$ EELS edges provide information on the unoccupied O-p, Mg-p, and Cu-d electronic densities of states, respectively [15]. The effect of the $2p$ core hole on the Cu L edge is minimal. While the $1s$ core holes on the O and Mg K edges distort the positions and intensities of the near-edge features, they do not introduce any new features at the 1 eV energy resolution used in this study (as we verified by comparison of *ab initio* calculations of the ground state density of states (DOS) to the EELS spectra). This allows a single-particle interpretation of the EELS spectra, which are proportional to local densities of states partitioned by site (as the incident probe is localized), chemical species (as

each element has unique core level binding energies), and angular momentum (from the dipole selection rules) [16,17]. In the STEM, the EELS measurements are made at internal interfaces, not free surfaces, which is achieved by passing the 100 keV electron beam (0.2–0.5 nm diameter) through a thin film. The interface is oriented parallel to the beam, so that a column of atoms in the interface plane can be measured separately from any atoms in adjacent columns.

To determine the chemistry of the {222} MgO/Cu interface, EELS spectra were recorded at and in the vicinity of the interface by scanning the beam over narrow strips of dimension 0.3×7 nm that run parallel to the interface. This technique minimizes the electron dose on the specimen, while maintaining the highest spatial resolution normal to the interface [14]. All spectra were acquired for 4 s or less, a dose 120 times less than the threshold for observable changes, thus avoiding any question of radiation damage at the interface. The specimen was tilted to a $\langle 110 \rangle$ orientation to place the {222} MgO/Cu interface parallel to the electron beam. Figure 1 shows an EELS composition profile across a {222} MgO/Cu interface. Each point on the plot corresponds to a 3 s exposure and was located by simultaneously recording the ADF signal. The integrated intensities from the O-K, Mg-K, and Cu $L_{2,3}$ edges were converted to concentrations using pure Cu and MgO as standards.

Figure 1 shows that an oxygen signal is present at the MgO/Cu interface, while the Mg signal is negligibly small. This indicates that this polar interface is O terminated, in accordance with the previous experimental data. Figure 2 shows the Cu $L_{2,3}$ edge recorded at the interface and in the bulk Cu. In contrast to previous studies of Cu/Al_2O_3 interfaces [18,19], we find no evidence for a Cu_2O electronic structure at the Cu/MgO interface. Instead, the copper retains the basic shape of the edge in that there is no sharp peak at the edge onset as might be expected for Cu_2O. As in Ni, the second peak on the Cu L_3 edge is the result of mixing of the free-electron-like DOS on the probed atom, with d states on neighboring atoms. At the interface, the number of d neighbors has been reduced, lowering the energy of the second peak to overlap with the first—a similar effect is seen in Ni-Al alloys [20]. A rough estimate of the charge transfer can be made by scaling the Cu L edges to the same intensity well above the edge onset. The area under each spectrum is now proportional to the number of d holes/Cu site [17,20], which are found to be the same for both the boundary and bulk spectra, to within experimental error (about 0.3 e^-/atom).

The change in the oxygen bonding is striking: we find a finite density of states throughout the unoccupied portion of the MgO band gap at the interface. Figure 3 shows the O-K edge recorded across the MgO/Cu interface. The large signal-to-noise ratios enabled deconvolution of the intrinsic spectra from the spectrometer point-spread function. This does not greatly alter any of the features, but makes the background subtraction much simpler. The edges collected at the interface appear much broader, with a well-pronounced prepeak on the bulk edge onset. The prepeak extends approximately 6 eV on the low-energy side (consistent with the unoccupied portion of the MgO band gap). The prepeak intensity decays rapidly with distance from the interface: 0.4 nm from the interface, it is almost gone. Fitting the prepeak intensity to an exponential yields a decay length of less than 0.3 nm. This should be viewed as an upper limit as the probe FWHM is 0.22 nm and probe tails decay inelastically with a 0.25 nm decay length [21]. Deconvolving the inelastic point spread function gives a decay length (averaged over the prepeak energies) of $\lambda_{\text{avg}} = 0.13 \pm 0.05$ nm. The

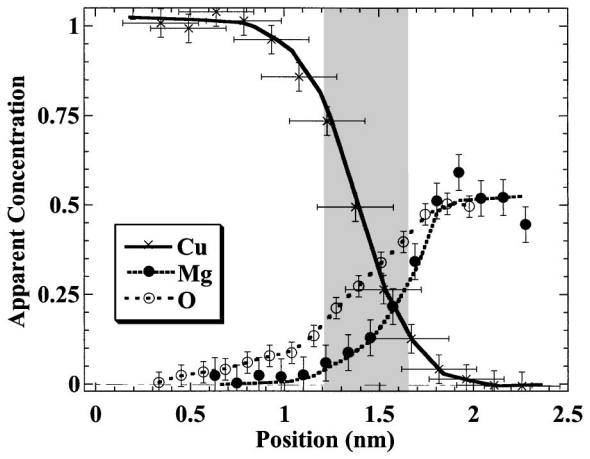

FIG. 1. EELS composition profile across a {222} MgO/Cu interface showing integrated intensities for Mg-K, O-K, and Cu $L_{2,3}$ edges, normalized to the bulk Cu and MgO signals. The O intensity at the interface is notably higher than Mg, showing that this polar interface is O terminated. The 90% width of the composition profile is 0.7 nm, and the 50% width is 0.3 nm. The spatial resolution is limited by incident probe diameter (0.25 nm), beam broadening inside the specimen (0.3 nm), and steps in the projected interface (± 0.243 nm).

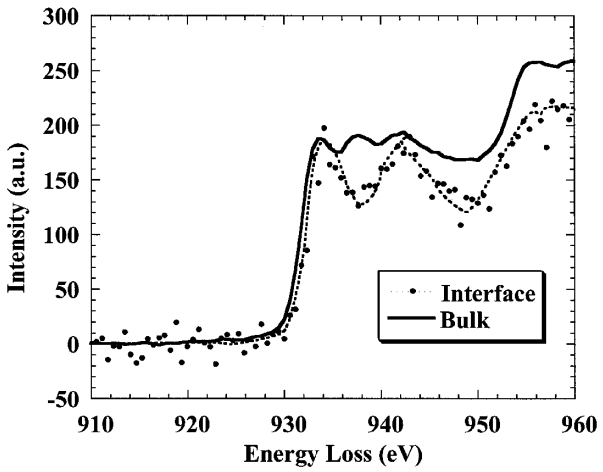

FIG. 2. Cu $L_{2,3}$ edge recorded at a {222} MgO/Cu interface and well away from the interface, in the bulk Cu.

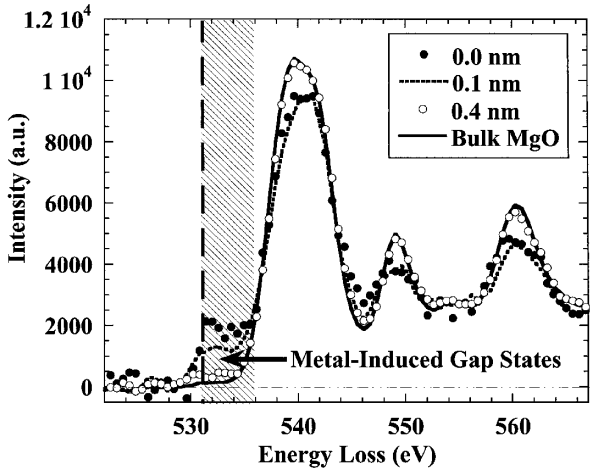

FIG. 3. O-K edges at various distances from a {222} MgO/Cu heterointerface. The "bulk" spectrum is taken from the center of the MgO precipitate (thick solid line). Spectra are scaled to match the post-edge background. The crosshatching marks the approximate position of the unoccupied portion of band gap in MgO.

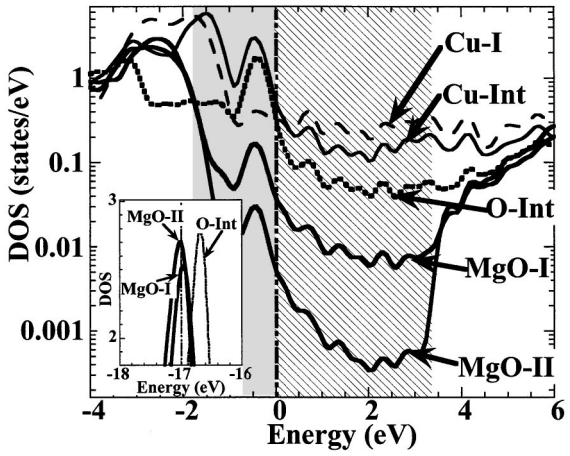

FIG. 4. Layer-projected electronic density of states in the vicinity of {222} MgO/Cu interface obtained by LDFT calculations. The zero of energy is the LDFT Fermi level. The shaded regions mark states in the bulk MgO gap, below the Fermi level. The crosshatched region indicates the empty portion of the MgO band gap (as in Fig. 3). The curves labeled "Cu-Int" and "O-Int" represent the Cu and the O layers at the interface, respectively. The curve labeled "Cu-I" represents the first Cu layer adjacent to the interface, while the curves labeled "MgO-I" and "MgO-II" represent the first and second MgO layers adjacent to the interface and show the development of the bulk band gap. The inset is a magnified view of the 0.2 eV shift of the O 2*s* states at the interface.

physical origin of this prepeak and its decay are discussed later in terms of metal-induced gap states.

Finally, the Mg-K edge was recorded in different locations across the interface. Within experimental error, the edge always retained the shape characteristic of bulk MgO. This is consistent with an O-terminated interface.

EELS has identified three key features at the {222} MgO/Cu interface: (i) that the interface is O terminated, (ii) that the number of *d* holes/Cu site is not significantly different from bulk Cu, implying that the interfacial Cu atoms remain almost neutral, and (iii) that there is a prepeak on the O-K edge, which is sufficiently broad in energy to remove the gap between the filled and empty oxygen states near the interface.

All three features are found in self-consistent, first principles, electronic structure calculations. We have examined the layer-projected densities of states of a coherent, oxygen-terminated {222} MgO/Cu interface calculated with plane-wave-pseudopotential local density functional theory (LDFT) [7,22]. In spite of the large misfit at the {222} MgO/Cu interface, coherent patches cover more than 50% of the interface area, and therefore calculations based on the coherent interface approximation are expected to yield useful insight into the true interface. The local density of states is integrated over slabs centered on each of the layers. While LDFT underestimates the width of the gap by 2–3 eV, the calculation of the offset of the MgO valence band with respect to the Cu involves only occupied states and is described accurately. Except for the layers adjoining the interface itself, the layers on both sides of the interface show relatively bulklike behavior (Fig. 4). The calculations show a shift of the O 2*s* band to a slightly higher energy at the interface, which reflects an electrostatic potential shift of roughly 0.2 eV. This is the expected interface dipole [7], which will alter the position of any core level with respect to the chemical potential, resulting in an EELS core level shift. From experiment we can place an upper limit on such shifts to less than 0.5 eV, which is consistent with the calculations, in being much smaller than the MgO band gap. The calculated layer-by-layer charge transfer does not exceed 0.18 e^-/atom. Another feature at the interface is a peak in the density of states at about 0.5 eV below the Fermi energy. It is most likely a hybrid of Cu 4*s* and O 2*p* states [23]. These states are occupied in the Cu/MgO system and cannot be measured with core loss EELS. At other transition metal/MgO interfaces, however, these states may be partially empty [24] and detectable with EELS.

More significantly, the layer-projected DOS for the O-terminated {222} MgO/Cu interface (Fig. 4) exhibit states in the MgO band gap, whose intensity decays exponentially with increasing distance from the interface. It is essentially the *p*-projected portion of these states that is responsible for the prepeak observed on the O-K edge. The characteristic decay length (which depends on the distance from the band edge), when averaged over the empty states, is $\lambda_{\text{avg}} = 0.11$ nm. While consistent with the experimental estimate of 0.13 ± 0.05 nm, the theoretical value should be regarded as an upper limit, as the LDFT underestimates the MgO band gap by 30%.

The O-K edge prepeaks, and the gap states which they reflect, can be qualitatively understood as metal-induced gap states [25,26]; they were first introduced for semiconductor/metal junctions, but are also applicable to

ceramic/metal interfaces [27,28]. The MIGS are the tails of the metal wave functions that decay exponentially into the insulating side of the interface. They are constructed from the conduction and valence bands of the insulator [27], as seen in Fig. 3 where intensity is transferred from the main O-K edge peak (the conduction band) to the prepeak (the MIGS). The decay length, $\lambda(E)$, is shorter for states that are farther in energy from the band edge. Thus in a large band gap material, the average decay length λ_{avg} ($\sim$0.1 nm in MgO) is smaller than in a small band gap semiconductor ($\sim$0.6 nm in Cu/Si [25]). Since the number of electrons in the MIGS is essentially constant [25], more states are concentrated at the interface for a wide-gap material than for a small-gap material. In wide-gap materials, the MIGS can more effectively supply electrons to compensate for the missing insulator neighbors—reducing the core level shifts between the interface and bulk. The interfacial metal atoms remain almost neutral as the MIGS electrons are supplied by the charge reservoir of the bulk metal, rather than the interface layer alone [25].

While the result of smaller core level shifts and charge redistributions at metal interfaces with large gap insulators (which are often considered ionic) than with semiconductors may seem counterintuitive if only electronegativity arguments are considered, this is a very reasonable result. Consider the limit where the band gap is made infinitely large: the metal can no longer couple to the insulator's conduction or valence bands, and instead resembles a free metal surface. The MIG wave functions have become the spillover of metal charge into the vacuum. For a metal such as Cu, the charge redistribution and resulting core level shift at a surface is small ($\approx$0.08 eV [29]). For the Cu/MgO simulations, we find the interface core level shift to be 0.2 eV, which is smaller than for a Cu/Si junction ($\approx$0.7 eV [25]).

In summary, we find the {222} MgO/Cu interface to be O terminated. Unlike a Cu monolayer on MgO, the bulk interface does not display a Cu_2O electronic structure. Instead, metal-induced gap states at the MgO side of the interface reduce charge redistributions at the interface and consequently the interface core level shifts as well. As noted by Finnis [28], MIGS should be a general feature of any ceramic/metal interface. LDFT calculations predict noticeable MIGS in Ag, Ti, and Al on (001) MgO [23,30–32]. It should be possible to observe MIGS at other interfaces between wide band gap materials and metals (or even small gap materials such as Si) as the decay of the tail of the metal wave functions into the insulator scales with the width of the band gap, rather than more subtle structural details such as orientation.

This research was supported by the U.S. Department of Energy (Grants No. DE-FG02-96ER45597 (Northwestern), No. DE-FG02-87ER45322 (Cornell), and Contract No. W-7405-ENG-48 at LLNL). The Cornell Materials Science Center STEM was operated and acquired with NSF Grants No. DMR-8314255 and No. DMR-9121654 and upgraded through AFOSR F49620-95-1-0427. The simulations were performed at the National Energy Research Supercomputer Center. Helpful discussions with P. Rez (Cu-O states by EELS), J. J. Rehr, and D. R. Hamann are acknowledged.

[1] *Proceedings of the International Symposium on Metal-Ceramic Interfaces*, edited by W. Mader and M. Rühle [Acta Metall. **40S**, 51–5368 (1992)].
[2] J. W. He and P. J. Møller, Surf. Sci. **178**, 934 (1986).
[3] I. Allstrup and P. J. Møller, Appl. Surf. Sci. **33**, 143 (1988).
[4] P. Lu and F. Cosandey, Ultramicroscopy **40**, 271 (1992).
[5] F. R. Chen *et al.*, Ultramicroscopy **54**, 179 (1994).
[6] H. Jang, D. N. Seidman, and K. L. Merkle, Interface Sci. **1**, 61 (1993).
[7] R. Benedek, M. Minkoff, and L. H. Yang, Phys. Rev. B **54**, 7697 (1996).
[8] F. N. Rhines, Trans. AIME **137**, 246 (1940).
[9] D. McMullan, P. Fallon, Y. Ito, and A. McGibbon, Proc. 10th Eur. Cong. Elect. Micr. (EUREM 92) **1**, 103 (1992).
[10] E. Kirkland, Ultramicroscopy **32**, 349 (1990).
[11] D. A. Muller, Y. Tzou, R. Raj, and J. Silcox, Nature (London) **366**, 725 (1993).
[12] D. A. Muller *et al.*, Phys. Rev. Lett. **75**, 4744 (1995).
[13] P. E. Batson, Nature (London) **366**, 728 (1993).
[14] N. D. Browning, M. M. Chisholm, and S. J. Pennycook, Nature (London) **366**, 143 (1993).
[15] R. F. Egerton, *Electron Energy Loss Spectroscopy in the Electron Microscope* (Plenum Press, New York, 1986).
[16] C. Colliex and B. Jouffrey, Philos. Mag. **25**, 491 (1972).
[17] J. E. Müller and J. Wilkins, Phys. Rev. B **29**, 4331 (1984).
[18] C. Scheu *et al.*, Microsc. Microanal. Microstruct. **6**, 19 (1995).
[19] R. Brydson *et al.*, Ultramicroscopy **59**, 81 (1995).
[20] D. A. Muller, D. J. Singh, and J. Silcox, Phys. Rev. B **57**, 8181 (1998).
[21] D. A. Muller and J. Silcox, Ultramicroscopy **59**, 195 (1995).
[22] R. Benedek, D. N. Seidman, and L. H. Yang, Microsc. Microanal. **3**, 333 (1997).
[23] Y. Li, D. C. Langreth, and M. R. Pederson, Phys. Rev. B **52**, 6067 (1995).
[24] P. Alemany, R. S. Boorse, J. M. Burlitch, and R. Hoffmann, J. Phys. Chem. **97**, 8464 (1993).
[25] V. Heine, Phys. Rev. **138**, A1689 (1965).
[26] S. Louie and M. Cohen, Phys. Rev. B **13**, 2461 (1976).
[27] C. Noguera and G. Bordier, J. Phys. III (France) **4**, 1851 (1994).
[28] M. W. Finnis, J. Phys. Condens. Matter **8**, 5811 (1996).
[29] P. Citrin and G. Wertheim, Phys. Rev. B **27**, 3176 (1983).
[30] U. Schönberger, O. K. Andersen, and M. Methfessel, Acta Metall. Mater. **40**, 1 (1992).
[31] C. Li, A. J. Freeman, and C. L. Fu, Phys. Rev. B **48**, 8317 (1993).
[32] T. Hong, J. R. Smith, and D. J. Srolovitz, Acta Metall. Mater. **43**, 2721 (1995).